SUBMISSION TO
GÉOTECHNIQUE LETTERS

DATE:
Written: 24th August 2021
Revised: 21st December 2021
Accepted: 11th January 2022

TITLE:
Structure evaluation of a tropical residual soil under wide range of compaction conditions

AUTHORS:
Bruna de Carvalho Faria Lima Lopes[a]
Vinícius de Oliveira Kühn[b]
Ângela Custódia Guimarães Queiroz[c]
Bernardo Caicedo[d]
Manoel Porfírio Cordão Neto[e]

AFFILIATION:
[a] University of Strathclyde, Department of Civil and Environmental Engineering, Glasgow, G1 1XJ, UK, ORCID: 0000-0001-7669-7236
[b] Universidade Federal do Oeste da Bahia, Centro das Ciências Exatas e Tecnologias, Barreiras, 47808-021, Brazil, ORCID: 0000-0001-5648-4372
[c] Instituto Federal de Goiás, Campus Anápolis, Anápolis, 75131-457, Brazil
[d] Universidad de Los Andes, Departamento de Ingeniería Civil y Ambiental, Bogotá, 111711, Colômbia, ORCID: 0000-0003-4344-0914
[e] Universidade de Brasília, Departamento de Engenharia Civil e Ambiental, Brasília, 70910-900, Brazil, ORCID: 0000-0003-0618-4376

CORRESPONDING AUTHOR:
Bruna de Carvalho Faria Lima Lopes
Department of Civil and Environmental Engineering
University of Strathclyde
James Weir Building - Level 5
75 Montrose Street - Glasgow G1 1XJ, Scotland, UK
E-mail: bruna.lopes@strath.ac.uk

KEYWORDS
compacted soils, residual soils, soil structure, pore size distribution, mercury intrusion porosimetry

Structure evaluation of a tropical residual soil under wide range of compaction conditions

Abstract

Soil compaction is one of the most common techniques used to engineer the soil. It is especially appealing to developing countries for its cost-effective and sustainable attributes for improving the soil's geotechnical characteristics. The compaction process along with the complexity of residual soils, abundant in the tropics zone, can have an impact on the performance of geotechnical structures built with these soils. Therefore, it is important to understand the influence that certain compaction conditions have on the structure of these materials. To investigate that, Mercury Intrusion Porosimetry tests were performed on compacted samples of a tropical residual soil from Brazil under different conditions of water content and compactive effort. Results show that the compacted soil under all studied conditions presents a bimodal Pore Size Distribution (PSD). It appears that the low availability of water within the macro-pores, hence suction, could have played a decisive role in maintaining the bimodal framework of the PSD. In this respect, the present study contributes to a better understanding of the tropical residual soils' structure when subjected to different compaction conditions, thus providing means to improve field applications.

Keywords:

Compacted Soils, Residual Soils, Soil Structure, Pore Size Distribution, Mercury Intrusion Porosimetry.

1. Introduction

Compaction is the soil state in which soils are mostly found when engineered. Indeed, most geotechnical infrastructures, such as embankments, containment structures and pavements, are typically built using local fine-grained soils, compacted to improve their hydro-mechanical characteristics (Kodikara, Islam & Sountharajah, 2018). This is the ideal sustainable approach, and an affordable solution to developing countries in the tropics zone, where residual soils have been historically engineered successfully based on experience, rather than systematic scientific studies (Wesley, 1990).

The aim of soil compaction is to ensure that the resulting earthwork possesses engineering properties that are adequate for the function of the enterprise (Craig, 2004). Soil compaction is then technically advised in order to: (i) increase stiffness hence reduce subsequent long-term and differential settlement under working loads; (ii) increase effective shear strength, therefore increase bearing capacity; and (iii) decrease void ratio and consequently reduce hydraulic conductivity (Selig, 1982). Thus, in practice, engineers rely on soil compaction specifications to deliver the required design properties. Unfortunately, the correlations between soil density and soil strength, stiffness and hydraulic conductivity are not universal. The impact compaction conditions have on the hydro-mechanical properties of the soil are related, amongst other things, to soil structure (Yokohama, Miura & Matsumura, 2014; Li, Shao & Vanapalli, 2020) and the fact that field compaction specifications are mostly related to soil density causes this point to be overlooked (Selig, 1982).

Therefore, given the importance of residual soils in compacted state, this paper aims at examining the influence of compaction conditions on the structure of a tropical residual soil from Brasília, Brazil. The compaction conditions assessed are those that in the field are often relaxed within a certain range determined by compaction specifications, such as water content, compactive effort and density. The soil fabric of the different samples is investigated by means of Mercury Intrusion Porosimetry (MIP) tests. Hence, this paper contributes to a better understanding of the engineering properties of tropical residual soils that predominate in vast parts of the planet and have been understudied.

2. Materials and methods

The tropical residual soil was collected at 1.7m depth from the Experimental Field of University of Brasília, Brazil. According to the Unified Soil Classification System (USCS) this material is classified as Low Plasticity Clay (CL). Characterisation experiments showed that liquid limit, w_L, is 42%; plastic limit, w_P, is 25%; plastic index, PI, is 17%; and specific gravity, Gs, is 2.73.

The three key compaction characteristics of the soil are the compaction energy, the water content and density. Thus, soil samples were prepared and grouped in a way that one of the variables of interest was isolated and the variations of the other two parameters could be observed.

In order to establish the points of interest, firstly the Standard Proctor compaction curve (Fig. 1a) of the material was determined. Then, points of interest were prepared by static compaction (Fig. 1a and b). For this, samples were air dried to the hygroscopic water content. Soil lumps were broken using a pestle and mortar. After that, a target amount of water was sprayed on the soil surface, and they were combined by manual mixing. Then the moist material was sieved (#10, 2mm) and sealed in a plastic bag for 24hrs for homogenisation. Static compaction was effected in three layers in an automated displacement control CBR equipment.

The compaction preparation method affects the fabric of the material, therefore samples prepared by static compaction have different fabric arrangement when compared with samples prepared under dynamic compaction conditions. Samples were grouped as follows:

- Group 1: Points compacted under the same energy (Standard Proctor), where A and B are on the dry of optimum, C is at optimum, D and E are on the wet of optimum. Standard laboratory compaction tests are conventionally performed to derive compaction field specifications. Thus, the objective of this group is to investigate the changes in the soil structure along the Standard Proctor compaction curve.
- Group 2: Points with the same dry unit weight (13.1 kN/m^3) compacted under different energies and varying water contents: A, F and H. It is common for compaction field specifications to establish water content values within an acceptable range; thus, this group aims at investigating the changes in the soil structure with the same density but having different water contents.
- Group 3: Points with the same dry unit weight (14.1 kN/m^3) compacted under different energies and varying water contents: G and D. This group has the same objective of Group 2; however, this group deals with a higher density, closer to that of the optimum point.
- Group 4: Samples at 21.5% water content (lower than optimum), compacted at different target void ratios (I1 to I4) under different compaction energies. Some compaction field specifications give contractors freedom to choose the most economical equipment and compaction process that render the desired density within the specified water content range. This effectively means that the compaction energy used could vary. Thus, the objective of this group is to investigate the changes in the soil structure with the same water content compacted under different energies.

- Group 5: Samples at 23.0% water content (at optimum), compacted at different target void ratios (J1 to J4), under different compaction energies. This group has the same objective of Group 4.
- Group 6: Samples at 23.9% water content (higher than optimum), compacted at different target void ratios (K1 to K4), under different compaction energies. This group has the same objective of Groups 4 and 5.

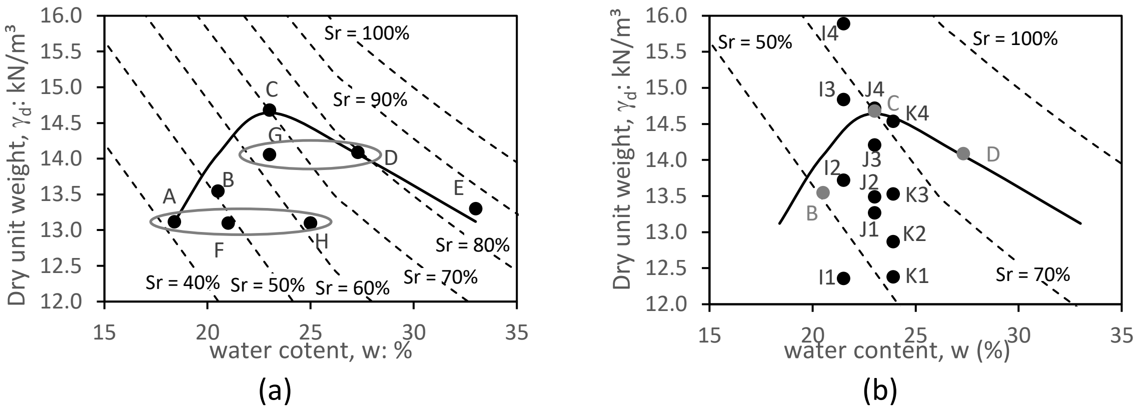

Fig. 1 Compaction curve and points of interest: (a) points defined by compaction curve and (b) points compacted under different compaction energies.

After defining the points of interest, all samples (Fig. 1a and b) were prepared for Mercury Intrusion Porosimetry (MIP) testing. Specimens of approximately 1 cm³ went through freeze-drying, by quickly freezing in liquid nitrogen followed by drying at vacuum oven (Otálvaro, Neto & Caicedo, 2015; Hernandez, Cordão Neto & Caicedo, 2018). MIP tests were carried out using AutoPore IV 9500 Micromeritics equipment, with nominal smallest pore diameter of 0.005 µm.

3. Results

Fig. 2 illustrates the differences observed between the void ratio of the samples (e_{SAMPLE}) and the final void ratio intruded by mercury during MIP tests (e_{MIP}). Results show that MIP tests performed on these samples tend to underestimate the void ratio of the sample within a 10%

margin (Fig. 2), which is similar to differences reported by other authors (Cordão Neto *et al.*, 2018; Delage & Lefebvre, 1984; Romero & Simms, 2008; Lloret *et al.*, 2003; Romero, 2013).

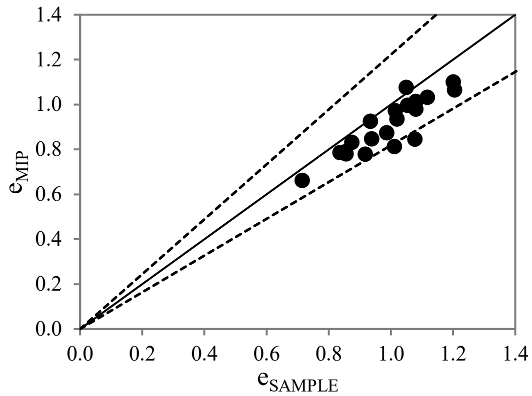

Fig. 2 Void ratio of sample and MIP, where full line is 1:1 and dashed lines are 10% tolerance span

Thus, to allow for a meaningful comparison of the compacted samples, the MIP intruded void ratio was normalized as follows.

$$e_{MIP}^{n} = e_{SAMPLE} \cdot \frac{e_i^{MIP}}{e_{MIP}} \qquad \text{Eq. 1}$$

where e^n_{MIP} is the normalized MIP void ratio; e_{SAMPLE} is the void ratio of the sample; e_i^{MIP} is the MIP void ratio associated with pore diameter *i*; and e_{MIP} is the final void ratio obtained by MIP test.

Additionally, the normalized cumulative MIP void ratio was fitted as suggested by Lopes et al. (2014) using 2 modes to represent the micro and macro porosity (Table 1). The two pore sizes void ratios are obtained by best fitting, in a way that $e^m + e^M = e^{MIP}$. Thus, the limiting diameter between macro and micro-pores is different from sample to sample.

Table 1 Bimodal fitting parameters for MIP tests, where e: void ratio, α and n: fitting parameters; *M* and *m:* refer to macro and micro, respectively.

Sample	**Group**	**w (%)**	**γ_d (kN/m^3)**	**e_{SAMPLE}**	**e^M**	**α^M (μm^{-1})**	**n^M**	**e^m**	**α^m (μm^{-1})**	**n^m**	**R^2**
A	1, 2	18.4	13.12	1.08	0.56	0.08	2.66	0.54	43.22	3.08	0.99
B	1	20.5	13.55	1.01	0.50	0.09	2.06	0.55	44.37	2.55	0.99
C	1	23.0	14.68	0.86	0.38	0.10	2.12	0.49	41.83	2.84	0.99
D	1, 3	27.3	14.09	0.93	0.51	0.31	1.56	0.45	40.54	2.73	0.99

E	1	33.0	13.30	1.05	0.64	0.27	1.55	0.42	40.23	2.99	1.00
F	2	21.0	13.10	1.08	0.60	0.04	3.22	0.54	50.54	2.12	0.99
G	3	23.0	14.06	0.94	0.44	0.06	2.69	0.55	47.87	2.28	0.99
H	2	25.0	13.10	1.08	0.53	0.04	2.72	0.66	77.44	1.72	0.99
I1	4	21.5	12.36	1.20	0.68	0.04	3.41	0.61	59.23	1.95	0.99
I2	4	21.5	13.72	0.99	0.47	0.07	2.97	0.57	48.28	2.20	0.99
I3	4	21.5	14.84	0.84	0.35	0.12	2.36	0.53	48.14	2.24	0.99
I4	4	21.5	15.89	0.71	0.28	0.29	1.70	0.45	40.91	3.16	1.00
J1	5	23.0	13.27	1.05	0.56	0.04	2.61	0.55	53.02	2.06	0.99
J2	5	23.0	13.49	1.02	0.46	0.06	2.55	0.54	57.48	1.97	0.99
J3	5	23.0	14.21	0.92	0.40	0.11	2.24	0.57	47.59	2.31	0.99
J4	5	23.0	14.72	0.85	0.37	0.12	2.05	0.51	43.54	2.56	0.99
K1	6	23.90	12.38	1.20	0.66	0.03	2.85	0.65	73.69	1.74	0.99
K2	6	23.9	12.87	1.12	0.57	0.04	3.33	0.67	80.26	1.69	0.99
K3	6	23.9	13.53	1.01	0.50	0.05	2.92	0.62	79.80	1.71	0.99
K4	6	23.9	14.54	0.87	0.40	0.12	2.25	0.53	53.27	2.13	0.99

3.1. Group 1 (A, B, C, D and E) – same compaction energy

Fig. 3a and b present Group 1's normalized MIP void ratio (Eq. 1) curve and the PSD of the fitted bimodal equation, respectively. The energy used to compact samples of Group 1 was roughly the same. However, each sample was prepared at different water contents and void ratios. The PSDs of all 5 samples are clearly bimodal, with micro-pores between 0.01 and 0.1µm and macro-pores ranging between 1 and 100µm. This is typical of tropical residual soils subjected to high chemical weathering and presence of natural aggregations (Futai & Almeida, 2005; Lopes, 2016; Otálvaro, Neto & Caicedo, 2015; Santos & Esquivel, 2018; Miguel & Bonder, 2012).

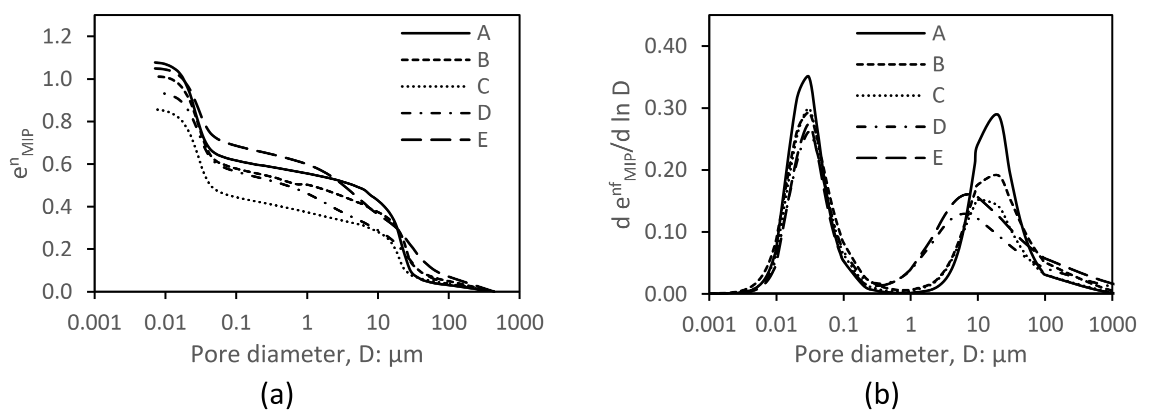

Fig. 3 MIP results of Group 1 samples on compaction curve (a) Normalized MIP, (b) Pore Size Distribution.

While the increase in water content seems to impact on the frequency and dominant pore size of the macro pores' range, it does not show much effect on the micro mode, apart from a small reduction in the frequency of the micro-pores.

3.2. Group 2 (A, F and H) and 3 (G and D) – same void ratio

Fig. 4 presents the normalized MIP void ratio (Eq. 1) curve and the PSD of samples in Groups 2 and 3. Samples in these two groups have the same dry unit weight, hence the same void ratio (Group 2: e_{SAMPLE} = 1.077; Group 3: e_{SAMPLE} = 0.938), but they were compacted at different water contents and using different compactive efforts.

The water contents of the samples go from lower than optimum (A and F for Group 2 and G for Group 3) to higher than optimum (H and D for Groups 2 and 3, respectively). The increase in water content did not affect the dominant micro-pores of samples in Group 2, only their frequency distribution was reduced. Meanwhile, the micro-porosity is virtually the same for samples in Group 3. The dominant macro-pores changed with the increase in water content for both groups. However, while in Group 2 the dominant macro-pores shifted to the right with the increase in water content, they shifted to the opposite direction, for Group 3 samples.

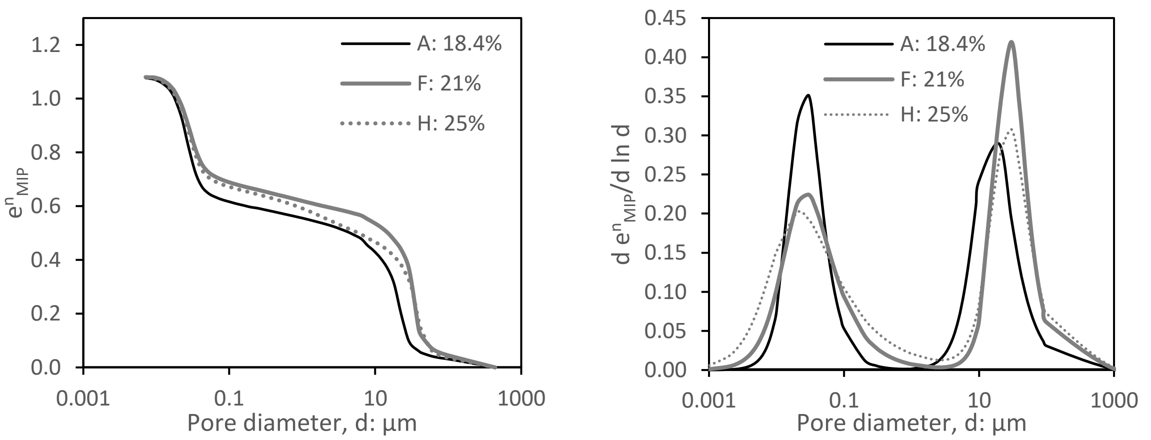

(a) (b)

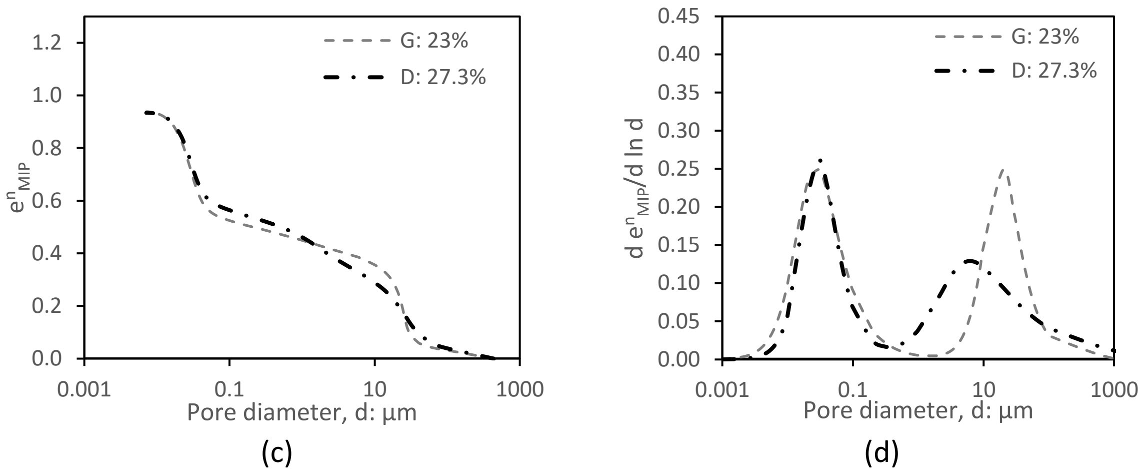

Fig. 4 MIP results of Group 2 samples (a) Normalized MIP; (b) Pore Size Distribution; MIP results of Group 3 samples (c) Normalized MIP; and (d) Pore Size Distribution.

3.3. Group 4 (I), 5 (J) and 6 (K) – same water content

Samples of Groups 4, 5 and 6 were compacted between them under the same water content but different compactive effort, which reflects the different void ratios obtained. Fig. 5 presents the normalized MIP void ratio (Eq. 1) curve and the PSD of samples in Groups 4, 5 and 6. In all cases the macro-pores density distribution reduces, and the dominant macro-pores shift to the left as the energy of compaction increases. Meanwhile, the dominant micro-pores do not change significantly. On the other hand, the density distribution of the micro-pores increases and becomes slightly narrower with the magnification of the compactive effort.

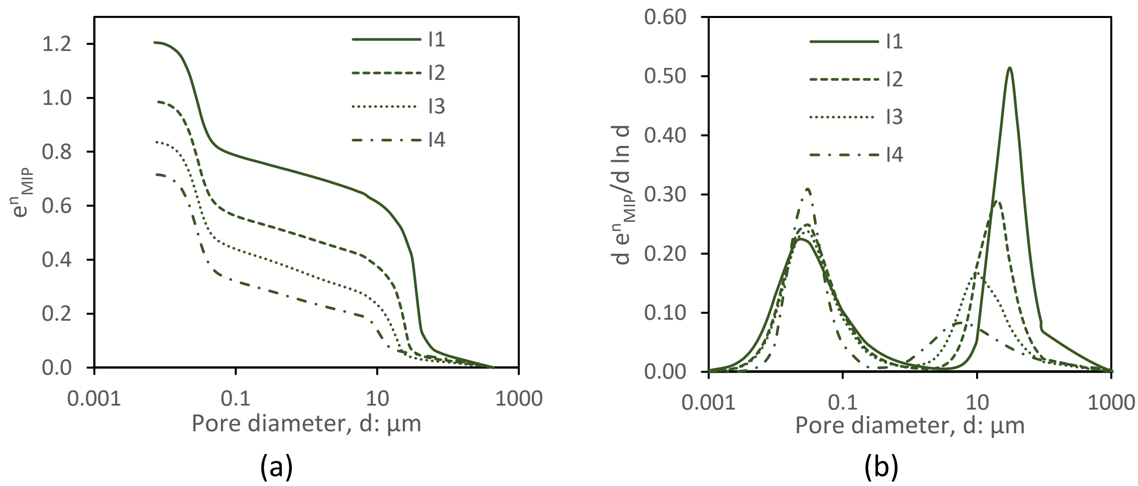

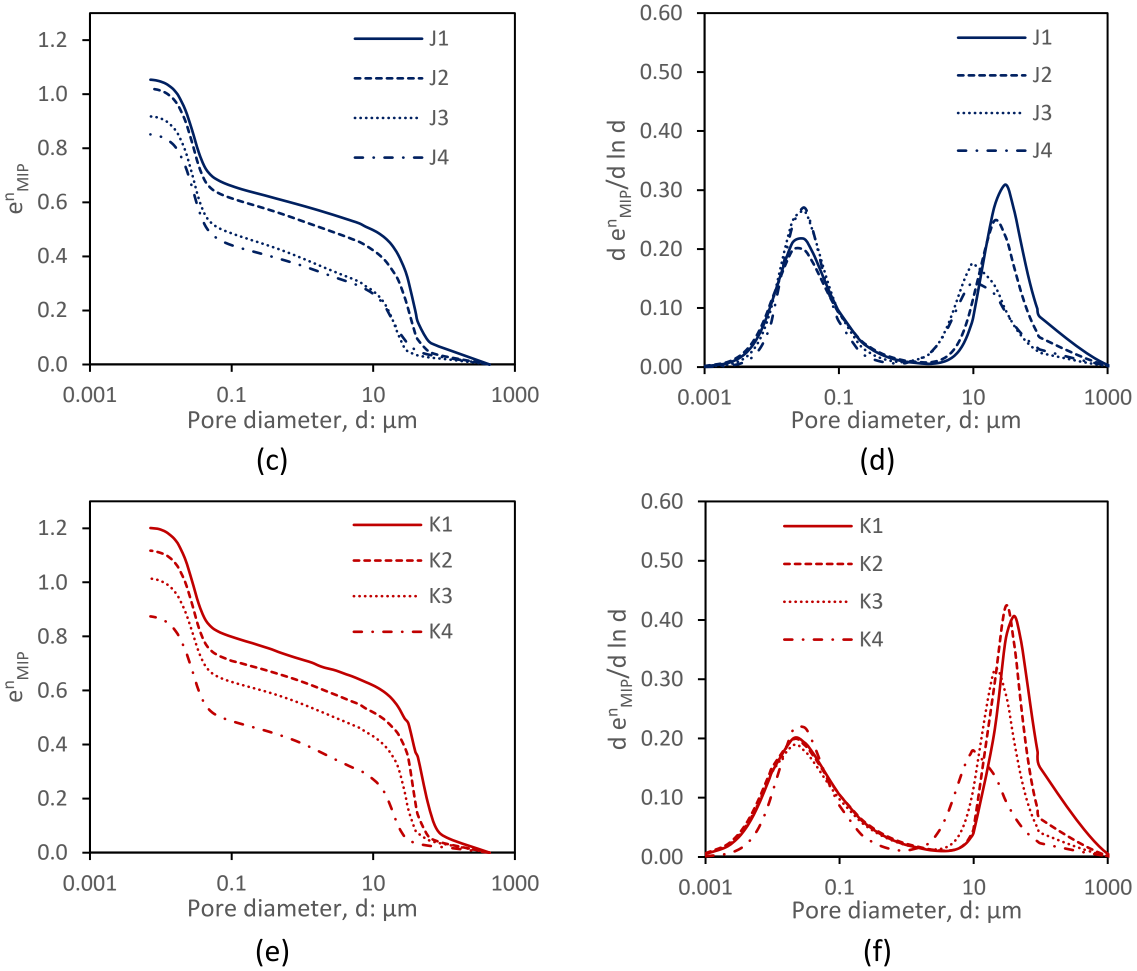

Fig. 5 MIP results of Group 4 samples (a) Normalized MIP, (b) Pore Size Distribution; MIP results of Group 5 samples (c) Normalized MIP, (d) Pore Size Distribution; MIP results of Group 6 samples (e) Normalized MIP, and (f) Pore Size Distribution.

4. Discussions

Compaction conditions affected the dominant macro-pore sizes while the dominant micro-pore sizes did not show significant variations in any of the groups. In fact, other authors have reported similar observations in these regards (Otálvaro, Neto & Caicedo, 2015; Santos & Esquivel, 2018). Queiroz (2015) determined experimentally the Soil Water Retention Curves (SWRC) for all the samples presented here. The SWRC of the samples fitted using a bimodal equation (Durner, 1994) are presented in the Appendix (Fig. A.1). Suction measurements obtained from this data were used to create the compaction plot with interpolated iso-suction curves (triangulation-based natural neighbour) presented in Fig. 6. On the dry side of optimum, the higher suction values seem to be more effective in keeping the size of dominant macro-pores than those on the wet of optimum. Suction appears to keep the aggregates resistant to the compaction process, thus it is necessary to increase the compactive effort to modify the dominant macro-pore size when the samples are on the dry of optimum, as observed for samples in Group 4. Indeed, this finding seems to be in line with Toll (2000)'s suggestion that the degree of aggregation of the data presented by Zein (1985) was related to the degree of saturation. The argument that suction supports the aggregated fabric raised in this paper is also consistent with evidence presented by Toll (1990) on a lateritic soil compacted at low degrees of saturation. The author suggested that the aggregated structure created by the low degree of saturation behaves like a 'coarser' material with a higher angle of shearing resistance.

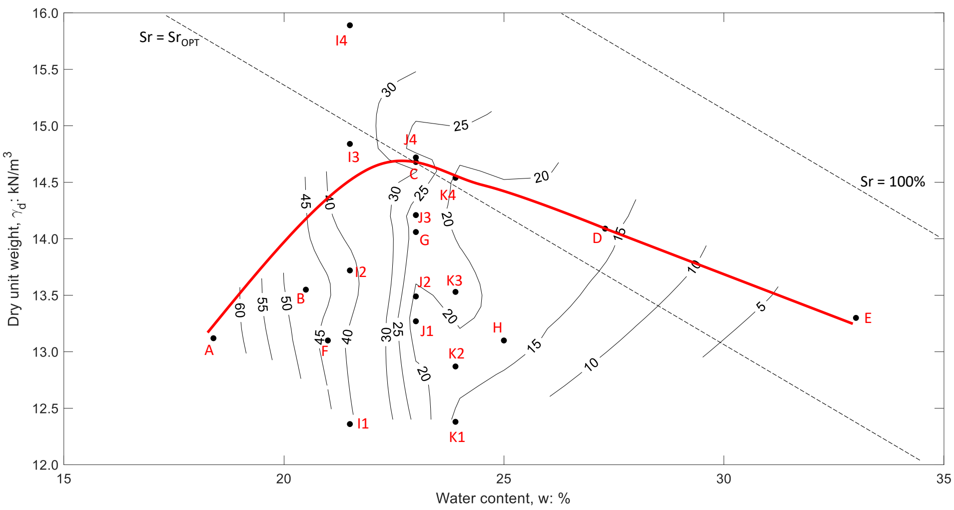

Fig. 6 Compaction plot with iso-suction curves.

The SWRC of the samples analysed (Fig. A.1) show that the micro-pores are fully saturated (Sr_m = 100%) at the given compaction water contents. Thus, the micro void ratio (e_m) can be used to estimate the water content of the micro porosity ($w_m = e_m/G_s$) hence the water content and the degree of saturation associated with the macro porosity can also be determined ($w_M = w_{sample} - w_m$; $Sr_M = w_M \times G_s/e_M$). Fig. 7 shows the compaction plot with interpolated iso-macro degree of saturation curves (triangulation-based natural neighbour). Apart from samples on the optimum (C), on the wet of optimum (D and E), and those compacted with the highest energy (I4, J4 and K4) the degree of saturation of the macro-pores of the other samples is very low, below 20%. Fig. 7 could help one understand the similar framework observed amongst the PSD curves of those samples below the Standard Proctor compaction curve. This plot (Fig. 7) suggests that the macro-pores of any sample under the Standard Proctor curve and on the dry side of the curve itself have very limited amounts of free water available, which in turn makes difficult for the macro-fabric to be modified.

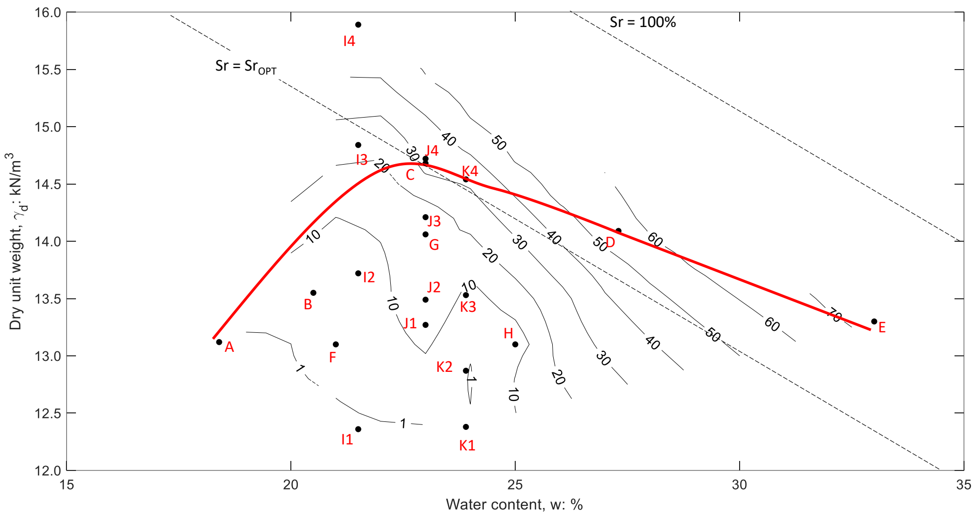

Fig. 7 Compaction plot with iso-macro degree of saturation curves.

5. Conclusions

This paper has investigated the influence that compaction conditions, such as water content, compaction energy and void ratio, have on the structure of a tropical residual soil. Results showed that the pore size distributions were affected by the different compaction conditions imposed on the samples. None of the different conditions of water content and energy imposed during compaction were sufficient to erase the macro-pores completely. In this sense, it appears that the low availability of water within the macro pores, hence suction, could have played a decisive role in maintaining the bimodal framework of the PSD.

Thus, the present study contributes to a better understanding of the evolution of one important engineering property, soil structure, of a historically understudied group of soils subjected to different compaction conditions.

Soil hydro-mechanical properties are directly related to soil structure. Further studies into this topic could provide aid to interpret the hydro-mechanical behaviour of soils, which affects the performance of geotechnical structures.

Data Availability Statement

All data and models that support the findings of this study are available from the corresponding author upon reasonable request.

Acknowledgments

The authors would like to thank Universidad de los Andes for the support provided to carry out the MIP tests.

References

Cordão Neto, M.P., Hernández, O., Lorenzo Reinaldo, R., Borges, C., et al. (2018) Study of the relationship between the hydromechanical soil behavior and microstructure of a structured soil. *Earth Sciences Research Journal*. [Online] 22 (2), 91–101. Available from: doi:10.15446/esrj.v22n2.65640.

Craig, R.F. (2004) *Craig's soil mechanics*. 447p. 7th edition. London, CRC Press/Balkema.

Delage, P. & Lefebvre, G. (1984) Study of the structure of a sensitive Champlain clay and of its evolution during consolidation. *Can. Geotech. J.* [Online] 21, 21–35. Available from: doi:10.1139/t84-003.

Durner, W. (1994) Hydraulic conductivity estimation for soils with heterogeneous pore structure. *Water Resourses Res.* [Online] (30), 211–223. Available from: doi:10.1029/93WR02676.

Futai, M.M. & Almeida, M.S.S. (2005) An experimental investigation of the mechanical behaviour of an unsaturated gneiss residual soil. *Géotechnique*. [Online] 55 (3), 201–213. Available from: doi:10.1680/geot.2005.55.3.201.

Hernandez, O., Cordão Neto, M.P. & Caicedo, B. (2018) Structural features and hydro-mechanical behaviour of a compacted andesitic volcanic soil. *Géotechnique Letters*. [Online] 8 (3), 195–200. Available from: doi:10.1680/jgele.18.00056.

Kodikara, J., Islam, T. & Sounthararajah, A. (2018) Review of soil compaction: History and recent developments. *Transportation Geotechnics*. [Online] 17 (September), 24–34. Available from: doi:10.1016/j.trgeo.2018.09.006.

Li, P., Shao, S. & Vanapalli, S.K. (2020) Characterizing and modeling the pore-size distribution evolution of a compacted loess during consolidation and shearing. *Journal of Soils and Sediments*. [Online] Available from: doi:10.1007/s11368-020-02621-3.

Lloret, A., Villar, M., Sanchez, M., Gens, A., et al. (2003) Mechanical behaviour of heavily compacted bentonite under high suction changes. *Géotechnique*. [Online] 53 (1), 27–40. Available from: doi:10.1680/geot.53.1.27.37258.

Lopes, B. de C.F.L. (2016) *Microstructural-based approach to the interpretation of clays and transitional soils behaviour*. 133p. PhD thesis. Departiment of Civil and Environmental Engineering. Universidade de Brasília, Brasilia, Brazil.

Lopes, B. de C.F.L., Tarantino, A. & Cordão Neto, M.P. (2014) An approach to detect micro- and macro-porosity from MIP data. In: N. Khalili, A. Khoshghalb, & Adrian R. Russell (eds.). *Unsaturated soils : research & applications : proceedings of the Sixth International Conference on Unsaturated Soils, UNSAT 2014*. 2014 Sydney, CRC Press/Balkema. pp. 685–690.

Miguel, M.G. & Bonder, B.H. (2012) Soil-Water Characteristic Curves Obtained for a Colluvial and Lateritic Soil Profile Considering the Macro and Micro Porosity. *Geotechnical and Geological Engineering*. [Online] 30 (6), 1405–1420. Available from: doi:10.1007/s10706-012-9545-y.

Otálvaro, I.F., Neto, M.P.C. & Caicedo, B. (2015) Compressibility and microstructure of compacted laterites. *Transportation Geotechnics*. [Online] 5, 20–34. Available from: doi:10.1016/j.trgeo.2015.09.005.

Queiroz, A.C.G. (2015) *Estudo do comportamento microestrutural de solos tropicais compactados*. 108p. PhD thesis. Department of Civil and Environmental Engineering.Universidade de Brasília, Brasilia, Brazil.

Romero, E. (2013) A microstructural insight into compacted clayey soils and their hydraulic properties. *Engineering Geology*. [Online] 165, 3–19. Available from: doi:10.1016/j.enggeo.2013.05.024.

Romero, E. & Simms, P.H. (2008) Microstructure investigation in unsaturated soils: A review with special attention to contribution of mercury intrusion porosimetry and environmental scanning electron microscopy. *Geotech. Geol. Eng.* [Online] 26 (6), 705–727. Available from: doi:10.1007/978-1-4020-8819-3_8.

Santos, R.A. dos & Esquivel, E.R. (2018) Saturated anisotropic hydraulic conductivity of a compacted lateritic soil. *Journal of Rock Mechanics and Geotechnical Engineering*. [Online] 10 (5), 986–991. Available from: doi:10.1016/j.jrmge.2018.04.005.

Selig, E.T. (1982) Compaction Procedures, Specifications, and Control Considerations. *Transportation Research Record 897: 1-8. National Research Council, Washington, DC, USA*.

Toll, D.G. (1990) A framework for unsaturated soil behaviour. *Géotechnique*. [Online] 40 (1), 31–44. Available from: doi:10.1680/geot.1990.40.1.31.

Toll, D.G. (2000) The Influence of Fabric on the Shear Behaviour of Unsaturated Compacted Soils. *Advances in Unsaturated Geotechnics*. [Online] 222–234. Available from: doi:10.1061/40510(287)15.

Wesley, L.D. (1990) Influence of Structure and Composition on Residual Soils. *J. Geotech. Engrg*. [Online] 116, 589–603. Available from: doi:10.1061/(ASCE)0733-9410(1990)116:4(589).

Yokohama, S., Miura, S. & Matsumura, S. (2014) Change in the hydromechanical characteristics of embankment material due to compaction state conditions. *Soils and Foundations*. [Online] 54 (4), 731–747. Available from: doi:10.1016/j.sandf.2014.06.010.

Zein, A.K.M. (1985) *Swelling Characteristics and Microfabric of Compacted Black Cotton Soil*. PhD thesis. Department of Civil and Environmental Engineering. University of Strathclyde, Glasgow, UK.

Appendix

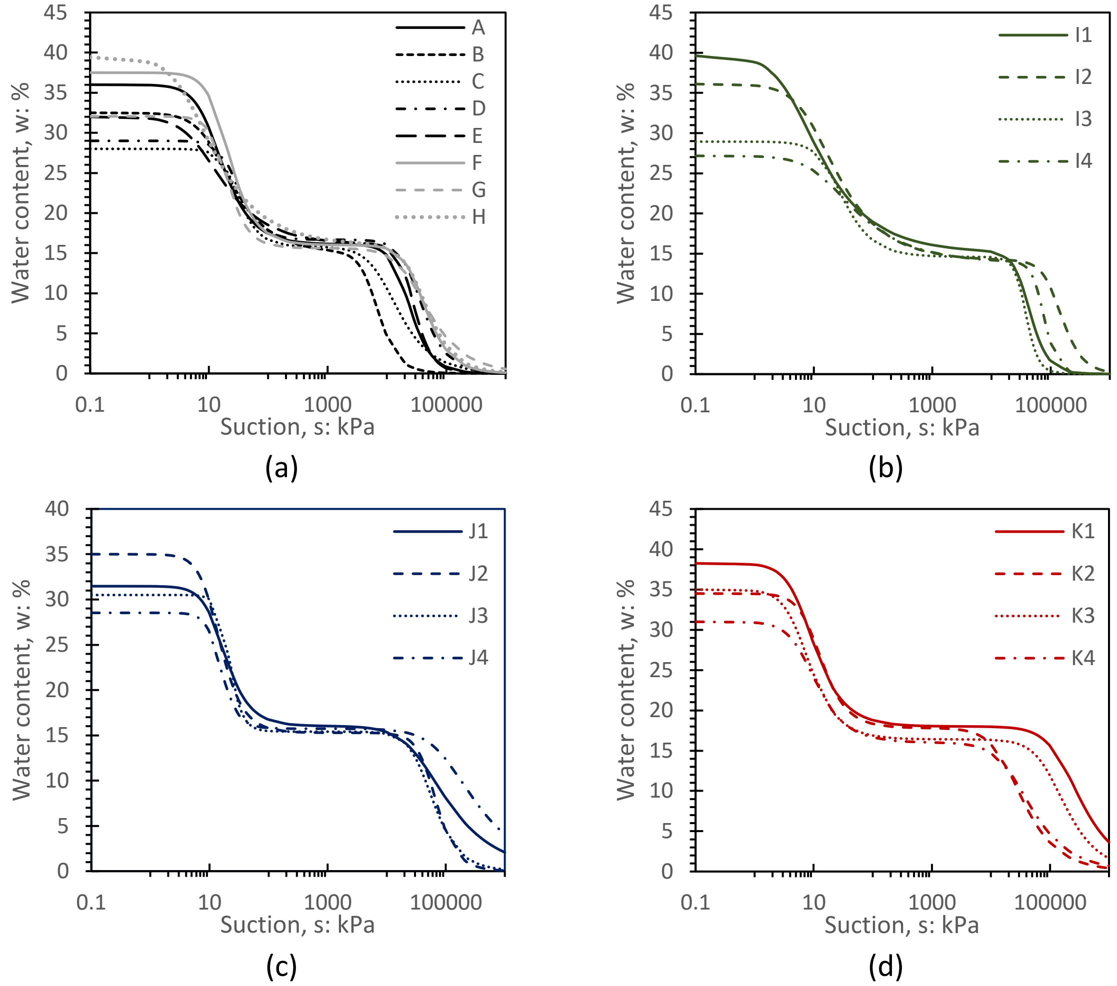

Fig. A.1. Soil-Water Retention Curves, samples in (a) Group 1 to 3, (b) Group 4, (c) Group 5, and (d) Group 6